Grid Voltage Control Analysis for Heavy-Duty Electric Vehicle Charging Stations

Preprint

Xiangqi Zhu, Rasel Mahmud, Barry Mather,
Partha Mishra, and Andrew Meintz

National Renewable Energy Laboratory

Presented at the 2021 IEEE Innovative Smart Grid Technologies, North America (ISGT NA)
February 15–18, 2021

NREL is a national laboratory of the U.S. Department of Energy
Office of Energy Efficiency & Renewable Energy
Operated by the Alliance for Sustainable Energy, LLC

This report is available at no cost from the National Renewable Energy Laboratory (NREL) at www.nrel.gov/publications.

Contract No. DE-AC36-08GO28308

Conference Paper
NREL/CP-5D00-77897
February 2021

Grid Voltage Control Analysis for Heavy-Duty Electric Vehicle Charging Stations

Preprint

Xiangqi Zhu, Rasel Mahmud, Barry Mather,
Partha Mishra, and Andrew Meintz

National Renewable Energy Laboratory

Suggested Citation
Zhu, Xiangqi, Rasel Mahmud, Barry Mather, Partha Mishra, and Andrew Meintz. 2021.
Grid Voltage Control Analysis for Heavy-Duty Electric Vehicle Charging Stations: Preprint.
Golden, CO: National Renewable Energy Laboratory. NREL/CP-5D00-77897.
https://www.nrel.gov/docs/fy21osti/77897.pdf.

NREL is a national laboratory of the U.S. Department of Energy
Office of Energy Efficiency & Renewable Energy
Operated by the Alliance for Sustainable Energy, LLC

This report is available at no cost from the National Renewable Energy Laboratory (NREL) at www.nrel.gov/publications.

Contract No. DE-AC36-08GO28308

Conference Paper
NREL/CP-5D00-77897
February 2021

National Renewable Energy Laboratory
15013 Denver West Parkway
Golden, CO 80401
303-275-3000 • www.nrel.gov

NOTICE

This work was authored in part by the National Renewable Energy Laboratory, operated by Alliance for Sustainable Energy, LLC, for the U.S. Department of Energy (DOE) under Contract No. DE-AC36-08GO28308. Funding provided by the U.S. Department of Energy Office of Energy Efficiency and Renewable Energy Vehicle Technologies Office via the 1+MW Medium Duty/Heavy Duty Vehicle Project. The views expressed herein do not necessarily represent the views of the DOE or the U.S. Government.

Grid Voltage Control Analysis for Heavy-Duty Electric Vehicle Charging Stations

Xiangqi Zhu, Rasel Mahmud, and Barry Mather
Power Systems Engineering Center
National Renewable Energy Laboratory
Golden, CO, USA
xiangqi.zhu@nrel.gov, rasel.mahmud@nrel.gov,
barry.mather@nrel.gov

Partha Mishra and Andrew Meintz
Center for Integrated Mobility Sciences
National Renewable Energy Laboratory
Golden, CO, USA
partha.mishra@nrel.gov, andrew.meintz@nrel.gov

***Abstract*— This paper presents an analysis of grid voltage control strategies for heavy-duty electric vehicle charging stations. The performance of three voltage control approaches—including power factor control, standardized volt-volt ampere reactive (VAR) curve control, and customized volt-VAR curve control—are investigated and evaluated for three different sizes of charging stations, including a single-port charging station, a midsized three-port charging station, and six-port travel center. The charging stations are placed on multiple locations of four different types of distribution systems to obtain a comprehensive performance analysis of the voltage control approaches under different scenarios. To quantitively compare the performance of the three voltage control approaches, a series of metrics are designed to quantify the performance and contribute to the comprehensive analysis.**

Keywords— heavy duty electric vehicle, charging station, voltage control, distribution system

I. Introduction

The electrification of heavy-duty vehicles is commencing, as electric vehicle (EV) companies achieve technology breakthroughs and bring cost-effective electric trucks to the market. Unlike light-duty EVs, electric trucks are equipped with very large batteries that have capacities over 400 kWh to account for higher power requirements over a similar distance of at least 200 miles. To maintain a reasonable charging time, charging stations for electric trucks require significantly higher charge rates than light duty vehicles and will induce heavy loads on the distribution system—up to a few megawatts if several trucks are charging together. These large loads generated by truck battery charging could cause significant voltage sags and high voltage ramps, which may limit charging station integration and/or increase grid interconnection costs. Therefore, it is important to understand the system voltage impact brought by heavy-duty EV charging loads and determine appropriate solutions for resolving or mitigating these impacts.

The current state-of-the-art research is mainly focused on the grid integration of light-duty EVs, with the target of using EV charging loads to achieve improved power system operation through a better understanding of EV behavior [1]–[4]. The system impact of heavy-duty EV charging loads and their associated resolutions have rarely been considered. In our previous work, we investigated the power system impact of heavy-duty EV charging stations at different locations of distribution systems [5] and found that voltage sags and high voltage ramps are critical concerns. Appropriate voltage control approaches are needed to resolve these issues.

In this paper we perform a comprehensive analysis of three representative voltage control approaches—including power factor control, standardized volt-volt ampere reactive (VAR) curve control, and customized volt-VAR curve control—to recognize the performance of the three approaches under various scenarios and determine which approach best fits which scenario.

We present four representative distribution systems for the analysis with varying characteristics. On each distribution system, we select multiple locations to connect charging stations, and we denote them as the best, good, and worst location according to their system impact, where the best has the least impact [5]. Three representative charging station sizes are selected: single-port, three-port, and six-port relating to how many heavy duty EVs can charge at any one given time. Recommendations on voltage control approaches for different scenarios and general guidelines for typical situations are derived from the comprehensive analysis.

The rest of this paper is organized as follows: Section II presents the voltage control approaches analyzed in this paper. Section III introduces the test systems. Section IV analyzes the simulation results, and Section V concludes the paper.

II. Voltage Control Approaches

This section introduces the three voltage control approaches: power factor control, standardized volt-VAR curve control, and customized volt-VAR curve control. All these approaches presume that the fast-charging equipment has the capability to use reactive power to help regulate the voltage.

A. Power Factor Control

To prevent deep voltage sag, negative power factor is applied to the inverter of the smart charger to let the power electronics components of the inverter work to inject reactive power to the grid to boost the voltage when the charger is pulling power from the grid. For easy hardware implementation, fixed power factor is usually used for this voltage regulating method, which means more reactive power will be generated if the load is higher.

B. Preset Volt-VAR Curve Control

Volt-VAR has been shown to be promising in providing voltage regulation for both higher and lower voltage conditions among all the voltage regulation modes [6]. In the latest edition

of IEEE Std. 1547-2018, a typical volt-VAR curve can be specified by four coordinate points in a volt-VAR plane, as shown in Fig. 1. IEEE Std. 1547-2018 recognizes two performance categories of distributed energy resources (DERs)—Category A and Category B—while specifying the volt-VAR requirements. Category B DERs have inherently more capability to modulate reactive power and have more stringent requirements than Category A DERs.

EV charging stations have been assumed to have a high level of grid capability and thus are Category B DERs because the charging stations are connected to the grid through inverters/active rectifiers. It is assumed that the nominal AC-side voltage, V_N, for the charging station is 1 p.u. The maximum reactive power, Q_{max}, that the charging station can generate or absorb is 44% of the charging station nameplate apparent power rating, S_{CS}^{rating}. The default settings in IEEE Std. 1547-2018 as shown in Table 1 are used in this study.

Table 1. Set points of the volt-VAR curve used in this study

Set points	(V_1, Q_1)	(V_2, Q_2)	(V_3, Q_3)	(V_4, Q_4)
Value	$(0.92\ pu, Q_{max})$	$(0.98\ pu, 0)$	$(0.98\ pu, 0)$	$(1.08\ pu, -Q_{max})$

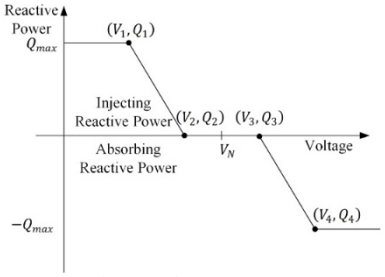

Fig. 1. Volt-VAR curve

C. Customized Volt-VAR Curve Control

Based on the voltage load sensitivity matrix (VLSM) developed in our previous work [7]–[8], we propose a customized volt-VAR curve control that will determine the amount of reactive power generation/absorption needed according to the voltage situation at different times of the day.

As shown in (1) and (2), $VLSM_P$ and $VLSM_Q$ represent the sensitivity matrix for the real and reactive power, respectively; and p_{ij} and q_{ij} are the sensitivity factors inside each matrix, which represent how much voltage will change at bus i if the real/reactive power changes at bus j.

$$|\delta V| = |VLSM_P||\delta P| + |VLSM_Q||\delta Q| \quad (1)$$

i.e.,

$$\begin{vmatrix}\delta V(1)\\ \vdots \\ \delta V(n)\end{vmatrix} = \begin{vmatrix}p_{11} & \cdots & p_{1n}\\ \vdots & \ddots & \vdots \\ p_{n1} & \cdots & p_{nn}\end{vmatrix}\begin{vmatrix}\delta P(1)\\ \vdots \\ \delta P(n)\end{vmatrix} + \begin{vmatrix}q_{11} & \cdots & q_{1n}\\ \vdots & \ddots & \vdots \\ q_{n1} & \cdots & q_{nn}\end{vmatrix}\begin{vmatrix}\delta Q(1)\\ \vdots \\ \delta Q(n)\end{vmatrix} \quad (2)$$

$$\delta V(i) = \sum_{j=1}^{n} p_{ij}\,\delta P(j) + \sum_{j=1}^{n} q_{ij}\,\delta Q(j) \quad (3)$$

From these three equations, the voltage changes, ΔV_i and ΔV_j, at buses i and j when the charging load, P_{charge}, is placed at bus i can be calculated by (4) and (5). Then we can obtain the relationship between the voltage change at buses i and j, as shown in (6). Through (7) and (8), the new voltage at bus j, (V_j'), can be represented by the original bus j voltage, V_j, and the voltage change at bus i. Substituting (8) into (9), we can calculate the minimum ΔV_i needed to maintain the voltage at bus j above the voltage limit, V_{limit}, as shown in (10) and (11).

By substituting (11) into (12), we can obtain the minimum voltage bus i needs to maintain, as shown in (13). Then, as shown in (14) and (15), by applying (13) for all the buses in the system, we can calculate the voltage that bus i needs to maintain to ensure that the voltages across the system are not less than V_{limit}. Then the reactive power needed on bus i at time t can be calculated by (16).

$$\Delta V_i = p_{ii} P_{charge} \quad (4)$$

$$\Delta V_j = p_{ji} P_{charge} \quad (5)$$

$$\Delta V_j = \Delta V_i p_{ji}/p_{ii} \quad (6)$$

$$V_j' = V_j + \Delta V_j \quad (7)$$

$$V_j' = V_j + \Delta V_i p_{ji}/p_{ii} \quad (8)$$

$$V_j' > V_{limit} \quad (9)$$

$$V_j + \Delta V_i \cdot p_{ji}/p_{ii} > V_{limit} \quad (10)$$

$$\Delta V_i > \left(V_{limit} - V_j\right) \cdot p_{ii}/p_{ji} \quad (11)$$

$$V_i' = V_i + \Delta V_i \quad (12)$$

$$V_i' > V_i + \left(V_{limit} - V_j\right) \cdot p_{ii}/p_{ji} \quad (13)$$

$$V_i' > V_i + \sum_{j=1}^{n}\left(V_{limit} - V_j\right) \cdot p_{ii}/p_{ji} \quad (14)$$

$$V_{ref} = V_i + \sum_{j=1}^{n}\left(V_{limit} - V_j\right) \cdot p_{ii}/p_{ji} \quad (15)$$

$$Q_i(t) = {(V(t) - V_{ref})}\Big/{q_{ii}} \quad (16)$$

III. Test System Preparation

A. Distribution System Preparation

To obtain a comprehensive understanding of the performance of the voltage control approaches, we prepared four representative distribution systems. As shown in Figs. 2–4, the IEEE 34-bus test system is used as a benchmark system [9], a utility-provided realistic single feeder is selected to represent single distribution systems, and a utility-provided realistic two-feeder distribution system is selected to represent multi-feeder systems. In addition, the realistic single feeder system is modified to develop a dedicated feeder where the substation is designed to power the charging station only, i.e. a potential method utility might use to serve such loads. Three locations are selected—best, good, and worst—to place the charging station based on the methods developed in our previous work [5].

Leveraging the load modeling methods developed in our previous work [10], all the feeders except for the dedicated feeder are all modeled with realistic load profiles. Instead of assigning each load bus with a profile scaled from the substation load, we model the load buses with load profiles that have appropriate diversities and variabilities to guarantee that load profiles for the test systems can have realistic diversity factors.

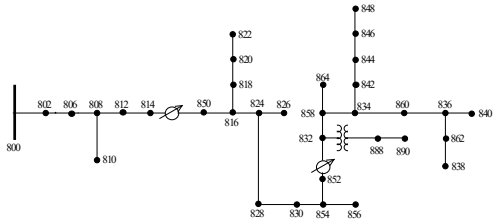

Fig. 2. IEEE 34-bus system [9]

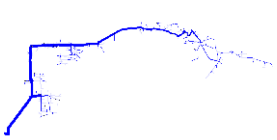

Fig. 3. Realistic single feeder

Fig. 4. Two-feeder system

B. Charging Station Modeling

This paper uses the EV, energy storage, and site optimization (EV-EnSite) tool to generate heavy-duty EV charging load profiles [11]-[12]. The EV-EnSite tool uses probability distributions of vehicle arrival schedule, initial states of charge (SOC) of the EVs, and different EV battery sizes to run Monte Carlo iterations emulating the charging behavior of populations of vehicles. These probability distributions are vehicle-type dependent and are developed using real-world vehicle telemetry data analysis for heavy-duty vehicles. An example of a vehicle arrival schedule at a station is shown in Fig. 5. The data are for a population of slightly more than 1,000 vehicles arriving at the station during 2 weeks at different times of the day. The density of the blue circles (o) and red triangles (Δ) at different times of the day shows the probability of a vehicle arriving at that time. Similarly, the histogram of initial SOC in Fig. 5 shows that although EVs with lower SOC have a higher probability to charge at a station, some EVs with higher SOC might stop and charge as well, emulating the behavior of drivers stopping at a rest stop. The charging stations simulated in this paper are en-route fast charging stations.

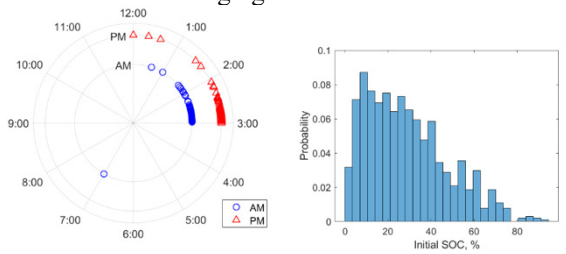

Fig. 5. (Left) Vehicle arrival time schedule at the station. (Right) Distribution of initial SOC of the vehicles

Once the vehicle arrival schedule and the corresponding vehicles (defined by their battery capacities and initial SOC) are initialized, the EV-EnSite tool simulates the vehicle arrival, queuing, and charging behavior of each vehicle over time at a particular station. A charging station is defined by the total number of charging ports, each port's power capacity, and the station's total power capacity. A vehicle is queued if a desired charging port is currently occupied; otherwise, it is plugged in and charged until a target SOC is reached. The charging power is limited either by the port's capacity or by limits imposed by the EV's battery management system.

In this paper, we analyze three different station configurations, each experiencing traffic of approximately 72 vehicles per day. We consider a single-port small charging station, a three-port midsize charging station, and a six-port travel center configuration, with each port providing a maximum power of 1.2 MW. The resulting EV charging load profiles are shown in Fig. 6. Although the peak and average charging load increase as the number of ports increase, such an increase might become necessary given the vehicle traffic because it affects the quality of service at the station. For example, a single-port station for 72 vehicles will result in days of wait time for most of the vehicles. Increasing the number of ports to three and six, however, results in a decreased average wait time from multiple days to 9 minutes and slightly less than 1 minute, respectively, thereby increasing the quality of service of the station.

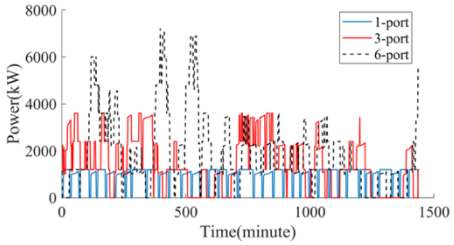

Fig. 6. EV charging load profiles for different station configurations

C. Analysis Metrics Design

As shown in Table 2, two metrics are designed to analyze the performance of the voltage control approaches: one for the voltage ramp and one for the voltage magnitude. To obtain the results in the entire simulation duration, the number of voltage ramps larger than the set limit and the number of voltage magnitudes lower than the set limit are recorded to summarize the percentage of the large ramp occurrences and the portion of the voltage sags. Here, the voltage ramp is calculated as $V(t) - V(t-1)$, where $V(t)$ and $V(t-1)$ represent the voltage at the current and previous steps.

Table 2. Analysis Metrics

Metrics	$V_{ramp} > r_{limit}$	$V < V_{limit}$
Definition	$n_{r-overlimit}/n_{ramp}$	$n_{v-overlimit}/n_{volt}$

IV. Simulation Results Analysis

This section discusses the simulation results of applying the three control approaches to different locations on the four representative distribution systems.

All the simulations are 1-week long with 1-minute resolution. The time-series voltage profiles are all for the first day, and the bar plots that demonstrate the analysis metrics described in Section III.C are the summarized results of all the buses on the test system for the 1-week simulation. Two negative power factors are applied for the power factor control: -0.9 and -0.8.

A. Results Analysis for IEEE 34-Bus Test System

Fig. 7 shows a one-day voltage profile of the node (one of the best locations) where the 6-port charging station is placed, . We can see that the voltage drop caused by the charging load is not significant, all within 0.01 p.u. Therefore, no voltage control is needed for this location if the charging station size is up to six ports. If considering a future expansion of this charging station, which would bring a higher charging peak load, then power factor control with a power factor of -0.9 and customized volt-VAR curve control are recommended. These two methods can help increase the voltage without causing extra voltage drops, which the volt-VAR curve control is doing, or extra voltage boosting, which -0.8 power factor control will do.

Figs. 8–9 show the 1-day voltage profile and 1-week statistical summary for the good location on the feeder. As shown in Fig. 8, the voltage drops to less than 0.9 p.u. on the

three-port charging station at the good location. Fig. 9 shows that the customized volt-VAR curve control performs the best in avoiding a large voltage drop and voltage sag. When there is only one charging port, the power factor control with -0.8 performs similarly to the customized volt-VAR curve control; however, when the charging station is expanded to six ports, the power factor control does not work well, but the performance of the standardized volt-VAR curve is comparable to that of the customized volt-VAR curve control.

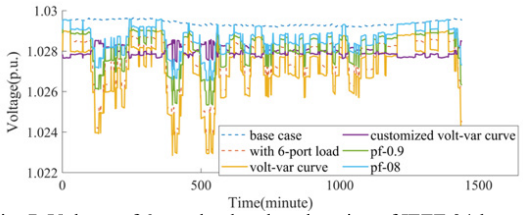

Fig. 7. Voltage of 6-port load on best location of IEEE 34-bus system

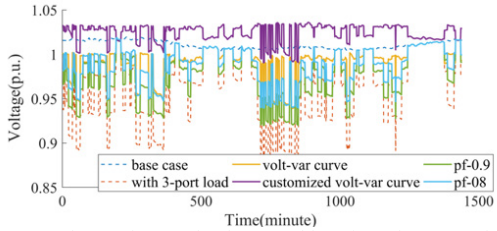

Fig. 8. Voltage of 3-port load on good location of IEEE 34-bus system

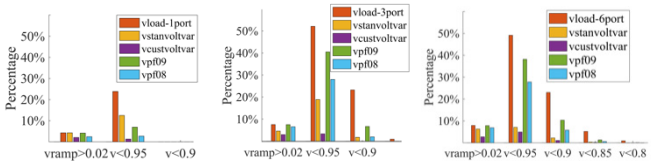

Fig. 9. Voltage analysis for good location of IEEE 34-bus system

Fig. 10 demonstrates the testing results for the worst location with a single-port charging station. This location cannot handle the three-port and six-port stations even with the voltage control approaches because of significant voltage sag. Fig. 10 shows that the customized volt-VAR curve control can barely maintain the voltage within the limit most of the time.

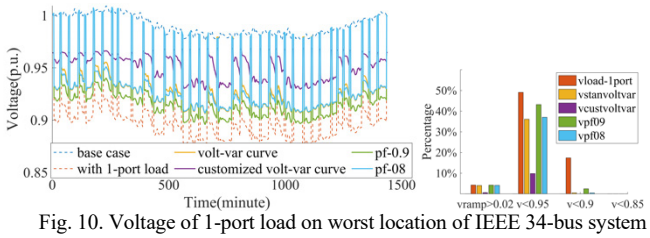

Fig. 10. Voltage of 1-port load on worst location of IEEE 34-bus system

B. *Results Analysis for Realistic Single Distribution System*

As Fig. 11 shows, the customized volt-VAR curve works best for the six-port charging station at the best location, whereas the other methods either lead to the voltage overshoots or do not reduce the voltage drops. The results are similar for the single- and three-port stations. Fig. 12 shows that all the control approaches can significantly reduce the number of occurrences when the voltage is less than 0.95 p.u. for the six-port charging station at the good location. Fig. 13 shows the results for the worst location with the three-port charging station, where the customized volt-VAR curve performs the best. This location cannot handle the six-port station without further mitigation efforts.

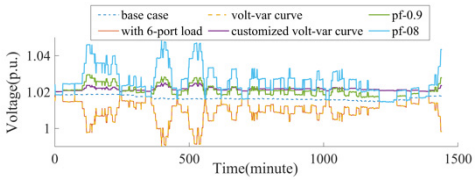

Fig. 11. Voltage of 6-port load on best location of realistic single feeder

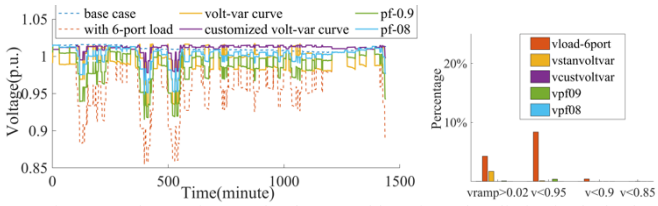

Fig. 12. Voltage of 6-port load on good location of realistic single feeder

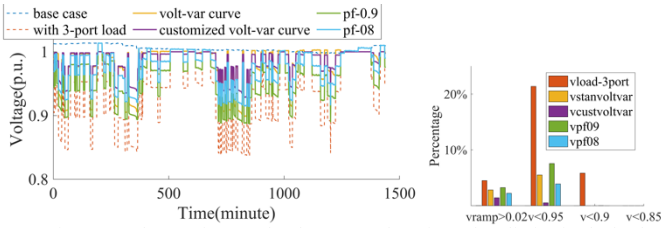

Fig. 13. Voltage of 3-port load on worst location of realistic single feeder

C. *Results Analysis for Dedicated Feeder Distribution System*

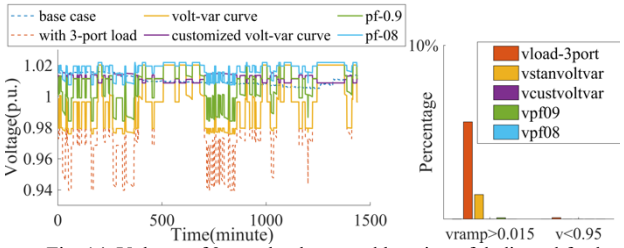

Fig. 14. Voltage of 3-port load on good location of dedicated feeder

We tested two locations on a dedicated feeder: 1) close to the substation (best); and 2) some distance from the substation (good). The customized volt-VAR curve control can help reduce the number of big voltage sags for the best location with the six-port load, whereas using the power factor control the voltage overshoots and using the standardized volt-VAR curve control does not take action because the voltage is within the deadband of the volt-VAR curve. As shown in Fig. 14 for the good location with the three-port load, all the control approaches can work well. The other methods perform better than the standardized volt-VAR curve control to reduce big voltage drops.

D. *Results Analysis for Two-Feeder System*

Similar to the single feeder and the dedicated feeder, the customized volt-VAR curve control performs better than the other two methods for the best location, whereas the power factor of -0.8 over boosts the voltage when providing voltage support. Fig. 15 demonstrates the analysis results for the good location with a six-port charging station. As shown, all the control methods work well except for the power factor control with -0.9.

Fig. 16 shows the summarized results for the worst location with different sizes of charging stations. All methods work for a single-port station, and the customized volt-VAR curve works

best for the three-port station. The customized and standardized volt-VAR curves have similar performance in reducing voltage sags for the six-port station; however, Fig. 17 shows that the standardized volt-VAR curve control over boosts the voltage when providing voltage support. Therefore, the customized volt-VAR curve is most suitable for the six-port station at the worst location.

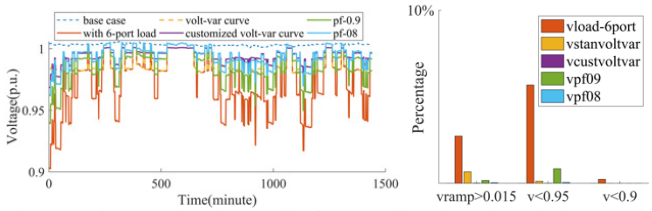

Fig. 15. Voltage results of 6-port load on good location of two-feeder system

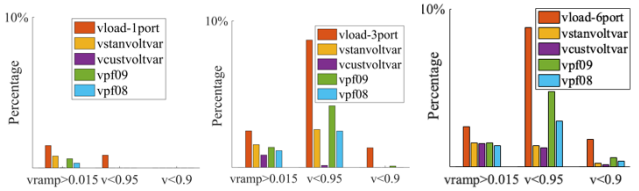

Fig. 16. Voltage analysis for worst location of two-feeder system

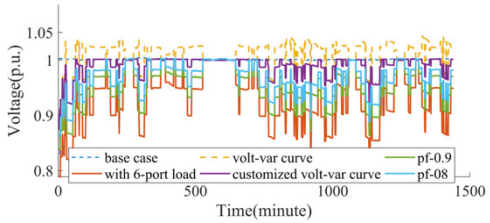

Fig.17. Voltage of 6-port load on worst location of two-feeder system

V. CONCLUSIONS

Table 3 summarizes the comprehensive analysis presented in this paper. In this table, a, b, c, and d represent the standardized volt-VAR curve, customized volt-VAR curve, power factor -0.8, and power factor -0.9, respectively; 1, 3, and 6 represent the single-port, three-port, and six-port charging stations, respectively. Table 3 shows that all the methods discussed in this paper can work for the best locations on different feeders as long as a low power factor, such as -0.8, can be avoided. Generally, the customized volt-VAR curve performs better than the other two methods, but when the charging station size is large, the standardized and customized volt-VAR curves have similar performance on boosting voltage (as shown in Fig 9 and 16), but the standardized volt-VAR curve may overboost voltage in some cases (as shown in Fig. 17). An insight that can be drawn from this is that the customized volt-VAR curve is recommended for fragile locations with small charging stations. A standardized volt-VAR curve is good enough for large station voltage controls.

Table 3. Analysis Summary

System Location	34-bus	Single feeder	Two-feeder	Dedicated feeder
Best	All work	c does not work for 6	c does not work for 6	c does not work for 6
Good	b works for 1 & 3; a & b work for 6	All work	d does not work for 6	All work
Worst	b works for 1; None work for 3 & 6	b works for 3; None work for 6	b work for 3; a & b work for 6	

ACKNOWLEDGMENTS

This work was authored by the National Renewable Energy Laboratory, operated by Alliance for Sustainable Energy, LLC, for the U.S. Department of Energy (DOE) under Contract No. DE-AC36-08GO28308. Funding provided by U.S. Department of Energy Office of Energy Efficiency and Renewable Energy Vehicle Technologies Office via the 1+ MW Medium Duty/Heavy Duty Vehicle Project. The views expressed in the article do not necessarily represent the views of the DOE or the U.S. Government. The U.S. Government retains and the publisher, by accepting the article for publication, acknowledges that the U.S. Government retains a nonexclusive, paid-up, irrevocable, worldwide license to publish or reproduce the published form of this work, or allow others to do so, for U.S. Government purposes.

REFERENCES

[1] Clement-Nyns, K., Haesen, E., & Driesen, J. (2009). The impact of charging plug-in hybrid electric vehicles on a residential distribution grid. IEEE Transactions on power systems, 25(1), 371-380.

[2] Richardson, D. B. (2013). Electric vehicles and the electric grid: A review of modeling approaches, Impacts, and renewable energy integration. Renewable and Sustainable Energy Reviews, 19, 247-254.

[3] Putrus, G. A., Suwanapingkarl, P., Johnston, D., Bentley, E. C., & Narayana, M. (2009, September). Impact of electric vehicles on power distribution networks. In 2009 IEEE Vehicle Power and Propulsion Conference (pp. 827-831). IEEE.

[4] Lopes, J. A. P., Soares, F. J., & Almeida, P. M. R. (2010). Integration of electric vehicles in the electric power system. Proceedings of the IEEE, 99(1), 168-183.

[5] Xiangqi Zhu, Barry Mather, and Partha Mishra, "Grid Impact Analysis of Heavy-Duty Electric Vehicle Charging Stations", submitted to 2020 IEEE Power & Energy Society Innovative Smart Grid Technologies Conference (ISGT). IEEE.

[6] Giraldez Miner, Julieta I., Hoke, Anderson F., Gotseff, Peter, Wunder, Nicholas D., Emmanuel, Michael, Latif, Aadil, Ifuku, Earle, Asano, Marc, Aukai, Thomas, Sasaki, Reid, and Blonsky, Michael. Advanced Inverter Voltage Controls: Simulation and Field Pilot Findings. United States: N. p., 2018. Web. doi:10.2172/1481102.

[7] Zhu, X., Wang, J., Lu, N., Samaan, N., Huang, R., & Ke, X. (2018). A hierarchical vlsm-based demand response strategy for coordinative voltage control between transmission and distribution systems. *IEEE Transactions on Smart Grid*, *10*(5), 4838-4847.

[8] Zhu, Xiangqi, and Barry Mather. "DWT-Based Aggregated Load Modeling and Evaluation for Quasi-Static Time-Series Simulation on Distribution Feeders." 2018 IEEE Power & Energy Society General Meeting (PESGM). IEEE, 2018.

[9] IEEE 34-bus Feeder, available online: https://site.ieee.org/pes-testfeeders/resources/

[10] Zhu, Xiangqi, and Barry Mather. "Data-Driven Distribution System Load Modeling for Quasi-Static Time-Series Simulation." IEEE Transactions on Smart Grid 11.2 (2019): 1556-1565.

[11] E. Y. Ucer, M. C. Kisacikoglu, F. Erden, A. Meintz and C. Rames, "Development of a DC fast charging station model for use with EV infrastructure projection tool," 2018 IEEE Transportation Electrification Conference and Expo (ITEC), Long Beach, CA, pp. 904-909, 2018.

[12] P. P. Mishra, E. Miller, S. Gupta, S. Santhanagopalan, K. Bennion, A. Meintz, and K. Walkowicz, "A framework to analyze the requirements of a multiport megawatt-level charging station for heavy-duty electric vehicles," presented in the 99th Annual Meeting Transportation Research Board, Washington DC, Jan 2020.